ME116 - Composite Materials Lab 1:

Fiberglass Laminate Testing

Thomas Iannelli

Benjamin Ledru

Joseph Skubic

Nicholas Yeung

March 13, 2026

Tufts University - School of Engineering

ME116

Abstract

Composite materials have become increasingly important across modern engineering industries, prompting the need for consistent predictive models validated against physical testing . In this study, 12-ply E-glass plain weave laminates were fabricated via vacuum bagging wet layups of two weave orientations, 0/90º and -45/45º. Theoretical laminate properties were predicted using the Rules of Mixtures (ROM) and Classical Lamination Theory (CLT), and structural behavior was further modeled using ANSYS Mechanical ADPL. Experimental results from INSTRON tensile testing were compared against these theoretical predictions, with fiber volume fraction (Vf = 0.34) used as a basis for the theoretical calculations. Theoretical predictions from ROM and CLT showed reasonable agreement with experimental results for the 0/90° laminate, with ANSYS strain error of only 5.29%, but diverged more significantly for the ±45° laminate, where off-axis shear-dominated behavior produced a strain error of 54.01%. Stress predictions were uniformly offset by 15.31% across both orientations due to a thickness discrepancy between INSTRON input assumptions and actual sample dimensions. The primary sources of discrepancy are attributed to an underestimated fiber volume fraction resulting from resin loss during vacuum bagging, the known limitations of iso-stress ROM assumptions for transverse and shear properties, and idealized boundary conditions in the finite element model. These findings highlight the importance of accounting for manufacturing variability when validating composite material models against experimental data.

1. Sample Manufacturing Process

The composite produced for this study was a 12-ply vacuum bagged wet layup composed of E-glass fiberglass and epoxy resin. Specifically, the fiber was Hexcel Hexforce 7532, plain weave, F16 finish, and the epoxy resin hardener mixture was Easy Composites EL2 and Easy Composites AT30 SLOW Hardener. Two layup samples were manufactured, notably on separate days, which may have led to inconsistencies with the vacuum seal of the layups to be discussed later. Relative to the weave direction, one sample had fibers oriented in the 0/90º position, and the other had fibers oriented in the -45/45º position. Both samples were 10 x 10 inch square flat panels, with a ply thickness of ~.0098 inches and total thickness of ~.118 inches.

The mass of fiber for both samples was found to be ~150 grams using a small scale. To achieve a 50:50 fiber to resin mass ratio, ~150 grams of resin mixture was measured according to the manufacturer's 10:3 resin to hardener ratio, which results in ~115 grams of epoxy resin and ~34 grams of hardener. To ensure the hardener was fully mixed in with the epoxy resin, the mixture was stirred slowly and continuously for five minutes, taking care to avoid air bubbles being introduced to the mixture, as these inclusions would negatively impact the final layup. The use of a slow hardener allowed for an extended pot life of up to 115 minutes, which guaranteed the resin mixture was not partially cured before completion of all layup layers.

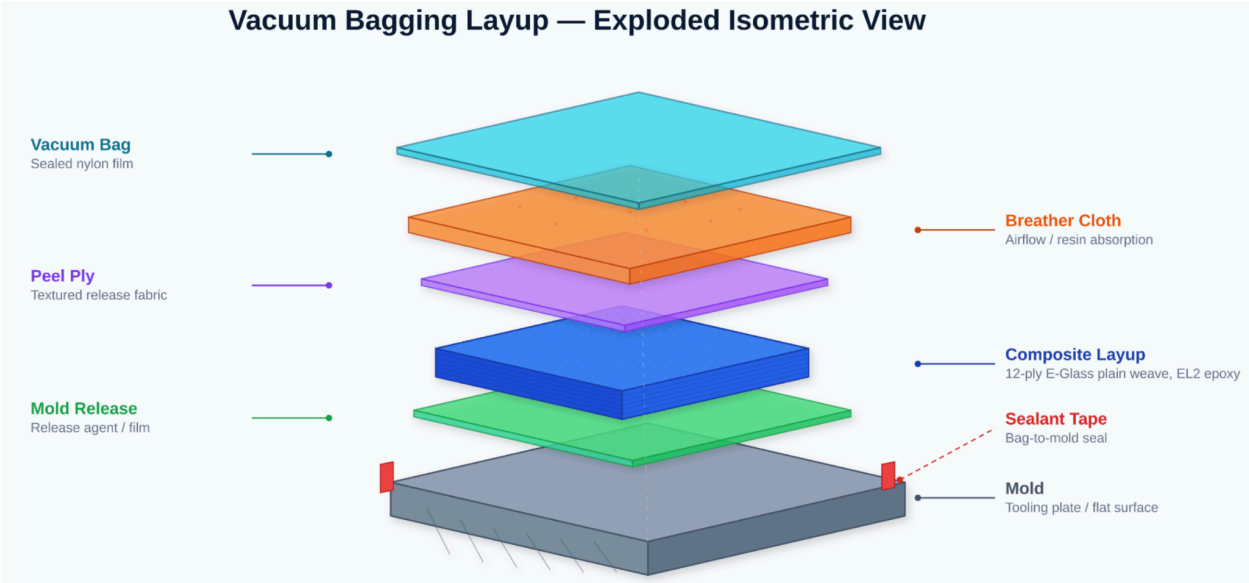

Figure 1. Exploded isometric view of vacuum bagging layup

As the study employs a vacuum bagged wet layup, a flat tooling plate is prepped with mold release to ensure the layup releases easily from the mold surface. For both samples, one ply of fiber was placed down, followed by a full wetting of said ply with the epoxy resin mixture before another ply was placed directly on top of the previous ply. This process was repeated for all 12 plies, making note of each sample's unique ply orientation. On top of the composite layup, an oversized peel ply layer was cut and placed to ensure a clean release from the above vacuum bagging material. This was followed by a 10 x 10 inch square of breather cloth, that enabled airflow once the part was under vacuum and absorbed excess resin from the composite layup that is drawn out under vacuum. Lastly, an airtight vacuum bag was adhered to the tooling plate with sealant tape, which ensures the part is under a strong vacuum for curing.

To complete the layup process, a vacuum tube is inserted through the vacuum bag and sealed with either a rubber gasket or more sealant tape. Then the vacuum is powered on, with attention being given to the seal of the layup. A proper vacuum seal is confirmed by visual cues like resin being drawn into the breather fabric and the bag adhering tightly to the tooling plate, as well as a clear and consistent pressure drop on the vacuum gauge. As per the cure schedule, the vacuum is left running until the resin reaches at least its gelation stage, which is after approximately 10 hours at 77ºF. Due to less than ideal temperature conditions in the lab, the vacuum can be left on for longer than this due to slower resin curing times, but there is the risk of too much resin being drawn out of the layup, which can lead to faults like delamination and dry spots in the final laminate. This can be resolved by using more resin during the layup process, but our study did not encounter any faults of this nature. The composite layup can be demolded from the tooling plate once it is completely cured after approximately 24 hours at 77ºF.

2. Rules of Mixtures

To predict the elastic properties of the manufactured laminate, the Rule of Mixtures (ROM) was applied at the ply level using the experimentally derived fiber volume fraction. The fiber volume fraction, Vf, was calculated from the measured fiber and resin masses and their respective densities, yielding 34% fiber by volume and 66% matrix by volume. Using published material properties from Hexcel for the fiber (Ef = 73.0 GPa, vf = 0.22) and Easy Composites for the resin (Em = 3.10 GPa, vm = 0.35), five composite properties were determined. The longitudinal modulus E1 and poisson's ratio v12 were calculated using the iso-strain (Voigt) assumption, while the transverse modulus E2 and shear modulus G12 were determined using the

iso-stress (Reuss) assumption. For the balanced plain weave of the Hexforce fabric, where fiber reinforcement is symmetric between the 0° and 90° directions, the effective laminate modulus was approximated as Ex = Ey = (E1 + E2)/2 for both samples. More properties can be calculated using the Rules of Mixtures, but for the purposes of this study, these five properties are sufficient. The resulting ROM predictions serve as the theoretical baseline against which experimental tensile results are later compared.

The fiber volume fraction was derived from the masses of the laminate materials measured during the manufacturing process and their published densities. For both samples, the fiber volume fraction was calculated as, $V_f = (m_f/\rho_f)/(m_f/\rho_f + m_m/\rho_m)$, where m_f and m_m are the fiber and matrix masses respectively (~150g), and $\rho_f = 2.55$ g/cm³ and $\rho_m = 1.15$ g/cm³ are their densities. This yields $V_f = 0.34$, meaning 34% of the laminate volume is occupied by fiber and the remaining $V_m = 0.66$ by matrix. It is worth noting that this V_f is notably lower than the 0.50–0.60 range typical of aerospace-grade laminates, which is expected for a wet layup process where precise resin control is difficult compared to prepreg manufacturing. This relatively resin-rich laminate is reflected in the ROM predictions and is an important factor when interpreting the comparison between theoretical and experimental results. Another crucial note is that these mass measurements are before vacuum bagging, so any resin drawn out during that process is not accounted for here, which will be discussed later.

With V_f and V_m, five composite properties can be derived using standard ROM formulas. The longitudinal modulus E1 determines behavior along the fiber direction and is

calculated under the iso-strain assumption, meaning fiber and matrix are assumed to deform equally in the loading direction:

$$E1 = Vf \cdot Ef + Vm \cdot Em = (0.34)(73.0) + (0.66)(3.10) = 26.87 \text{ GPa}$$

The transverse modulus E2 controls behavior perpendicular to the fiber direction and is calculated under the iso-stress assumption, where fiber and matrix carry equal stress but deform independently:

$$1/E2 = Vf/Ef + Vm/Em \rightarrow E2 = 4.60 \text{ GPa}$$

Poisson's ratio ν12 describes the transverse contraction resulting from longitudinal loading and follows the same iso-strain mixture rule as E1:

$$\nu12 = Vf \cdot \nu f + Vm \cdot \nu m = (0.34)(0.22) + (0.66)(0.35) = 0.306$$

The in-plane shear modulus G12 is calculated analogously to E2 under the iso-stress assumption, using the constituent shear moduli derived from their elastic constants and Poisson's ratios:

$$1/G12 = Vf/(Ef/2(1+\nu f)) + Vm/(Em/2(1+\nu m)) \rightarrow G12 = 1.70 \text{ GPa}$$

Because the fiber used, HexForce 7532, is a balanced plain weave fabric, reinforcement is equally distributed in the 0° and 90° directions within each ply. As a result, the laminate behaves quasi-isotropically in the plane and the effective extensional modulus in both the x and y directions can be approximated as average of the longitudinal and transverse ply moduli:

$$Ex = Ey \approx (E1 + E2)/2 = (26.87 + 4.60)/2 = 15.73 \text{ GPa}$$

It should be noted that this is a simplification of the laminate moduli. A full CLT analysis using the ABD matrix provides a more rigorous prediction of laminate stiffness, particularly for the ±45° specimens where off-axis coupling effects become significant. Nevertheless, this ROM derived laminate modulus provides a useful estimate and a straightforward benchmark for comparison with experimental tensile modulus values extracted from INSTRON testing.

3. Sample Preparation Process

Once our 12-ply fiberglass layups finished curing during vacuum-bagging, they were ready to be cut into individual test samples. Several machines exist to cut out samples, but the waterjet was chosen because laser cutting can cause the fiberglass to release toxic fumes and can yield uneven cutting of the glass fibers, which is a safety hazard. The waterjet is the ProtoMAX machine manufactured by OMAX, and uses a combination of high pressure water extruded through a nozzle and abrasive sand to cut 2D geometry through flat sheets of high-strength materials. To ensure consistency during testing across all materials and sample types, and to allow for generalization of our results by adhering to engineering standards, the American Society of Testing and Materials (ASTM) D3039 standard was followed. Unlike for testing of standard polymers, this standard dictates a rectangular, constant cross-section test bar with a length of 10in, a width of 1in, and a thickness of 3mm, or 0.118in. OnShape, a cloud-based CAD software, was used to create a 2D sketch of the test bar, which was then exported as a .dxf file into the waterjet's ProtoMAX software.

Figure 2. ProtoMAX Waterjet

The fiberglass layup plate was fastened flat in the waterjet at the four corners using clamps, water was added until it covered the part, the nozzle was calibrated using the calibration stand-off, and a dry-run was conducted to ensure no collisions between the nozzle and the clamps. Once everything was checked over, the full run was conducted and 3 samples were cut out from the 12-ply sheet. This was repeated across both fiber orientations to obtain 6 samples (3 samples for the 90 laminate, and 3 for the 45 laminate).

Figure 3. Fiberglass Samples (45 and 90 orientations) Pre-testing

4. INSTRON Testing Process

To begin, a test method was defined in the Instron machine which defines the key testing parameters that the machine will follow. The strain rate of the sample was fixed to 3 mm/min (tensile tests can range from 1 to 50 mm/min), and the end condition for the test was set to when the applied load drops below 95% of the initial load. This value was obtained through trial and error—since there were several composite materials being tested, the initial end condition of 80% drop in load wasn't enough to capture failure in all four materials, and therefore we increased it to 95%. This lengthened the tests but ensured we saw physical failure in all test samples across all materials. Moreover, this trial and error also allowed us to define 4 mm of displacement as a threshold to remove the extensometer which collects strain data, as this sensor

is very costly and has a maximum displacement which, if surpassed, will cause permanent damage. Finally, the sample dimensions were measured using calipers and included in this test method in order for the machine to provide accurate stress and strain calculations.

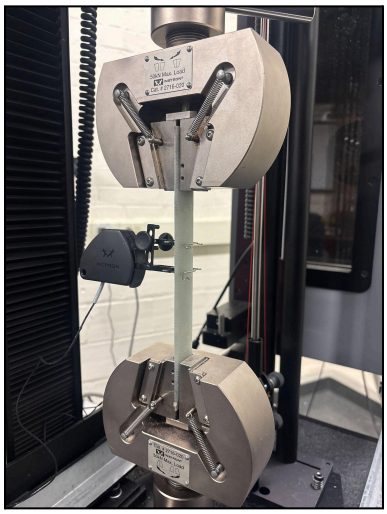

Figure 4. Fiberglass Sample During Testing (with Strain Gauge)

With a test method complete, samples are then clamped at both ends by the jaws and the strain gauge is mounted on the middle of the gauge length. The strain gauge is then calibrated, the force reading is zeroed, and testing is begun. Once displacement reaches 4 mm, the strain gauge is removed and the test is continued until sample fracture. This process is repeated for all samples, and then force-displacement and stress-strain data is exported onto a USB drive. The post-testing samples are shown below, with the orientation of the fibers having a visible effect on the fracture mechanics of the sample. The 0/90 laminate fractures normal to the applied load direction, whereas the 45 laminate fractures at a 45 degree angle from the loading direction in all 3 samples. This is quite neat!

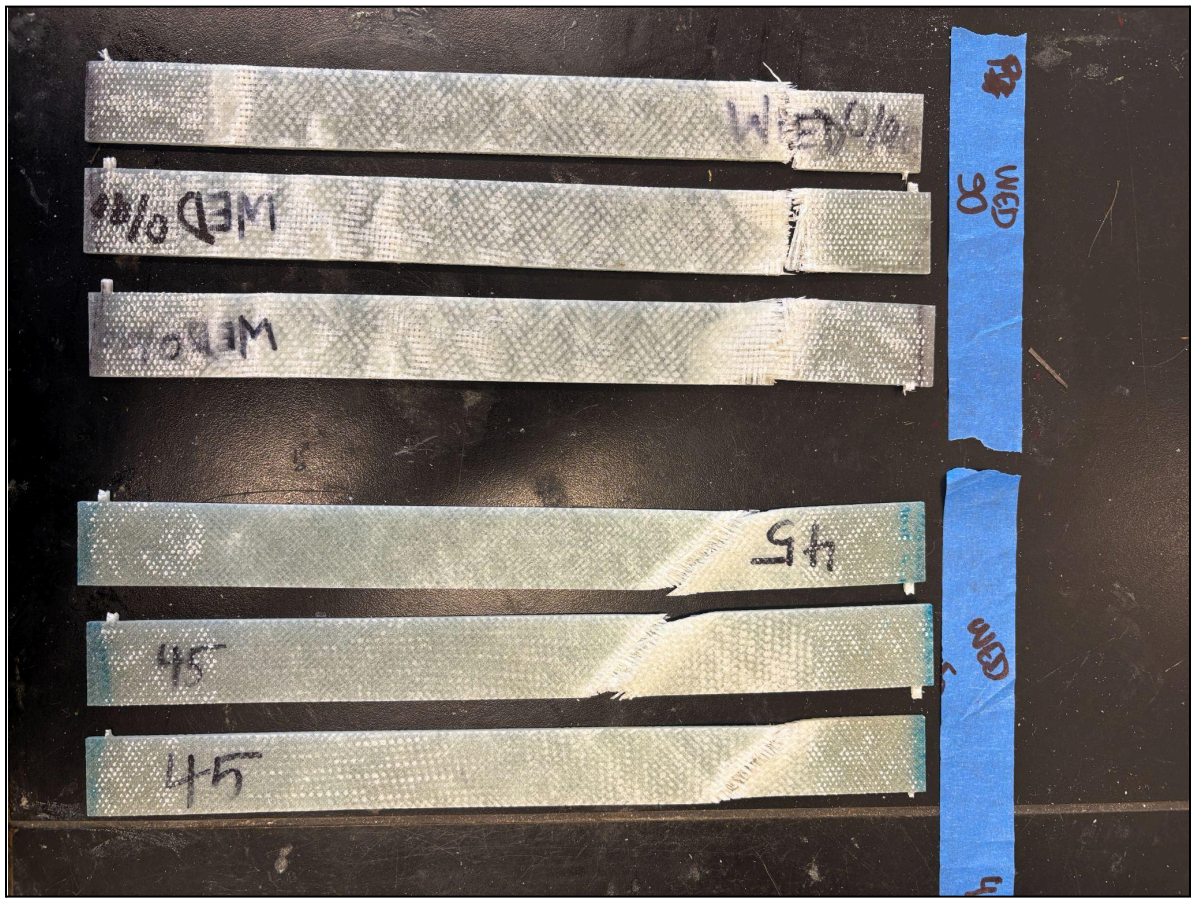

Figure 5. Samples Post-Test

During testing, the strain gauge occasionally malfunctioned and yielded obsolete data. Fortunately, one sample of each orientation yielded high-quality strain data, which is plotted below alongside Force-Displacement profiles for all four samples.

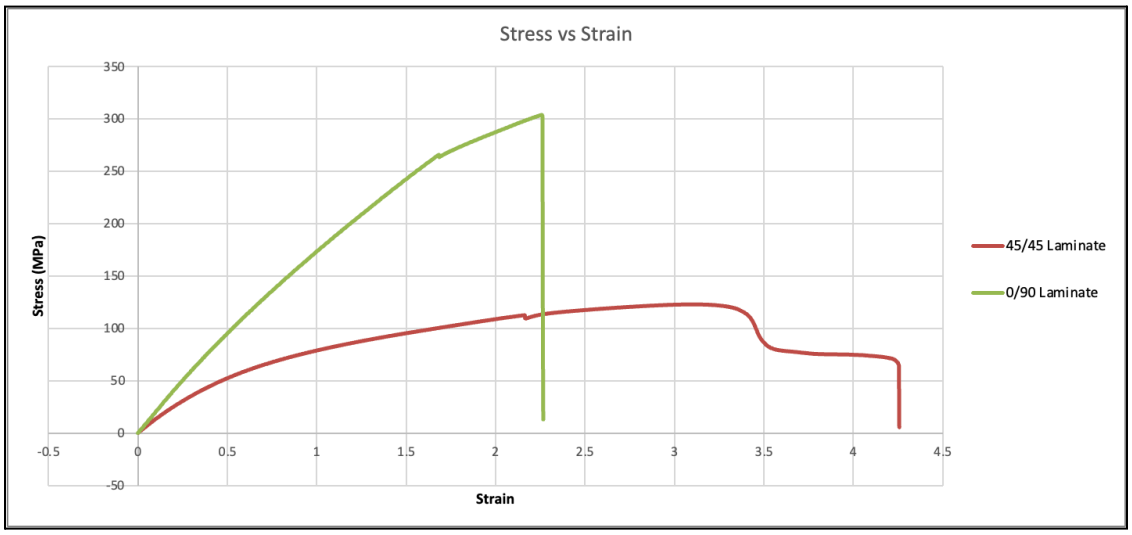

Figure 6. Stress-Strain Profile for Samples with Usable Strain Data

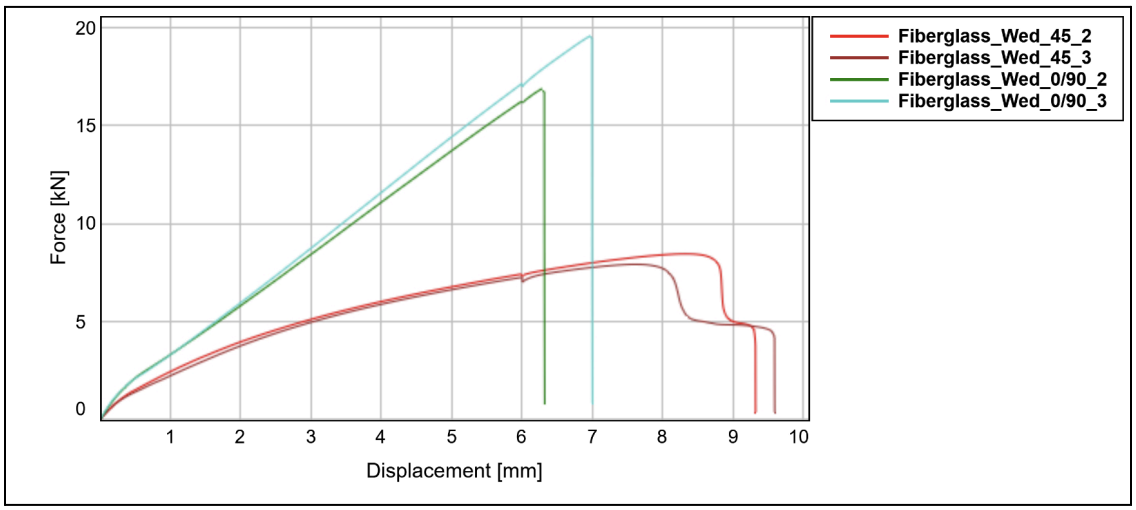

Figure 7. Force-Displacement for All Samples

Moreover, the Instron machine uses constitutive relationships (Hooke's Law), the 0.2% offset, and user inputs for sample dimensions in order to calculate UTS, yield strength, and Young's Modulus across every test with valid strain data. Instron calculations for these material properties

were averaged across samples and a standard deviation was calculated to quantify variability. This is also displayed below in table format.

45° Laminate	INSTRON	
	Mean	*Standard Deviation*
Modulus (E)	12.495 GPa	0.365 MPa
Ultimate Tensile Strength (σ_{UTS})	124.947 MPa	17.064 MPa
Yield Strength (σ_Y)	66.33 MPa	1.89 MPa
90° Laminate		
Modulus (Ef)	19.675 GPa	0.215 MPa
Ultimate Tensile Strength (σ_{UTS})	284.216 MPa	4.431 MPa
Yield Strength (σ_Y)	202.15 MPa	0.66 MPa

Figure 8. Calculated Mean Material Properties and Standard Deviation for Instron Testing

5. Discussion of Instron Testing Results & Variability

From data above, it can be noted that the 90° laminate has higher strength and modulus than the 45° one, reflected in that UTS, yield strength, and Young's Modulus are greater in the fiber direction for the 90° laminate. However, the 45° laminate has higher toughness and is more ductile, meaning it has a greater area under the curve (can withstand more stress and strain and therefore absorb more energy, before failure) and fails at a significantly greater value of strain. Each laminate orientation therefore offers benefits and drawbacks depending on the loading

condition. A part with a 90° orientation would benefit if loading was primarily in bending or pure tension, but a 45° would be preferable for torsional loading.

It can also be noted that the 45° laminate has higher variability, or standard deviation from the mean, on average. This is especially true of the UTS standard deviation, which is greater than that of the 90° laminate by a factor of 4, and most likely comes down to there being a difference in quality between samples that caused failure under much different stress levels. Other factors during the testing process beyond sample preparation are potential contributors to variability in measured properties. For example, slight misalignment in how the sample is loaded into the test grip that may not be readily visible to the user can vary the true loading direction slightly between tests. Similarly, slippage at the grips can cause the sample to stretch less than the jaws have actually displaced vertically, yielding slightly erroneous data and possibly prompting the end of the test before the sample has fractured. Since these would typically occur later in the test, variability (standard deviation) for properties calculated in the linear elastic region is much lower than that of the UTS for both laminates.

6. ANSYS Analysis

Finite element analysis was performed using ANSYS Mechanical APDL 2025 R2 to predict the tensile response of the composite laminate coupons under axial loading. Simulations were conducted for both the 90° and 45° laminate configurations using the same load level selected from the experimental Instron data. The primary outputs considered were total displacement, tensile strain, and tensile stress. These values were then compared with the

corresponding experimental results at 3 kN in order to evaluate how well the model represented the physical coupon behavior.

The key experimental and ANSYS results are summarized in Table 1, while the percent differences between the numerical and experimental values are shown in Table 2. Representative ANSYS contour plots for displacement, strain, and stress are provided in Figure 1 for the 90° laminate and Figure 2 for the 45° laminate.

Table 1. Comparison of Instron and ANSYS results at 3 kN

Laminate	Source	Force (kN)	Displacement (mm)	Tensile Strain (%)	Tensile Stress (MPa)	Thickness (mm)
90°	Instron	3	0.8594	0.2376	46.4961	2.54
90°	ANSYS	3	0.5728	0.2504	39.3788	3
45°	Instron	3	1.3221	0.4301	46.4998	2.54
45°	ANSYS	3	1.5143	0.6624	39.3788	3

Table 2. Percent difference between ANSYS and experimental results

Laminate	Displacement Difference (%)	Strain Difference (%)	Stress Difference (%)	Thickness Difference (%)
90°	33.35	5.29	15.31	18.11
45°	14.54	54.01	15.31	18.11

Figure 9. ANSYS displacement, tensile strain, and tensile stress contours for the 90° laminate.

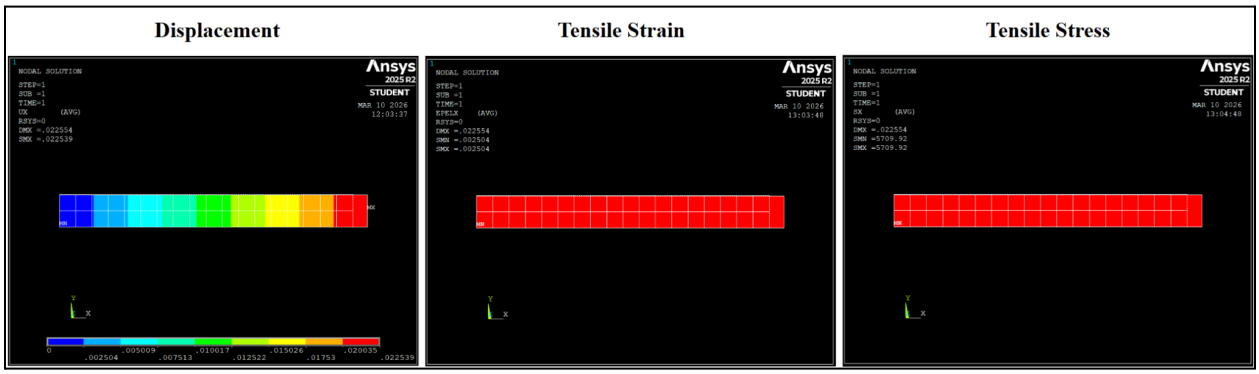

Figure 10. ANSYS displacement, tensile strain, and tensile stress contours for the 45° laminate.

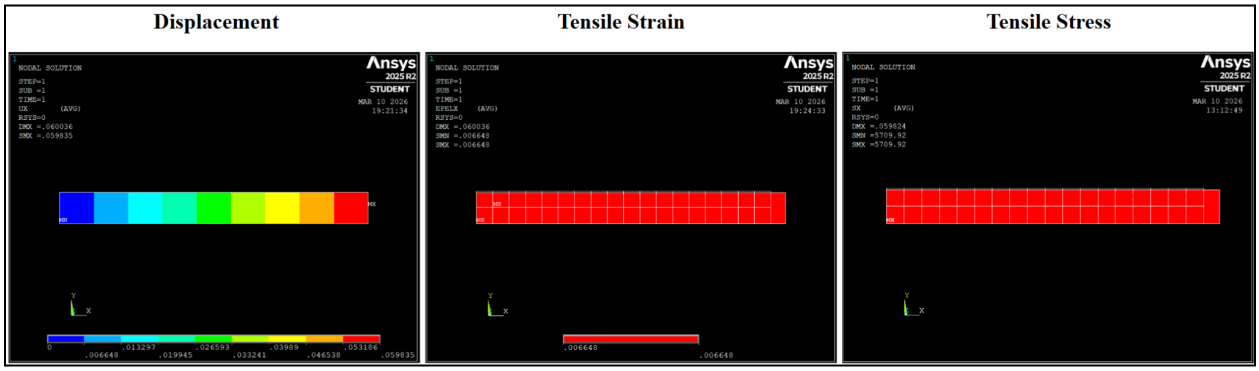

The ANSYS results showed reasonable agreement with the experimental data in some areas, but the accuracy depended on laminate orientation. The 90° laminate showed the closest agreement in tensile strain, with a percent difference of only 5.29%, indicating that the model captured this response relatively well. In contrast, the 45° laminate showed a much larger difference in strain, with an error of 54.01%, suggesting that the off-axis laminate response was not represented as accurately.

The displacement predictions followed a similar trend. For the 90° laminate, the ANSYS model underpredicted displacement, while for the 45° laminate it slightly overpredicted displacement. The trend is reasonable because the 90° and 45° laminates carry the load

differently. The 90° laminate behaves more simply under direct axial loads and so a model that is ideal will be too stiff and so underpredict displacement. The 45° laminate experiences shear effects and so the previously stated potential inaccuracies in the off-axis and shear-related material properties have most likely led to the bloated displacement.

The stress values predicted by ANSYS were also lower than the experimental values for both laminates, with the same percent difference in each case. Because both models were evaluated under the same applied load, the difference here comes from an assumption of the test thickness of 2.54 mm in intron testing when the actual sample was 3mm.

Several additional factors likely contributed to the difference between simulation and experiment. The numerical model assumed idealized material behavior, geometry, and boundary conditions, whereas the experimental coupons were subject to real manufacturing variation, Instron gripping effects, and possible material nonuniformity.

Overall, the ANSYS Mechanical APDL 2025 R2 model captured the general tensile response of the laminate coupons, but the level of agreement varied between the two laminate orientations. The results indicate that the model represented the 90° laminate more accurately than the 45° laminate, particularly in terms of strain. Improved results would likely require using the measured coupon thickness in the original Instron test, more accurate experimentally derived material properties, and boundary conditions that more closely match the actual Instron test setup.

7. MATLAB Analysis

Classical Laminate Theory (CLT), a series of mathematical calculations used to predict how composites behave under various loads and moments, was executed through the use of MATLAB. From knowing the longitudinal modulus (E_1), transverse modulus (E_2), shear modulus (G_{12}), poisson's ratio (ν_{12}), as well as the applied loads (N) and moments (M) on the composite, CLT is able to output the reduced stiffness matrix (Q), the transformed stiffness matrix ($\bar{Q}$), the extensional stiffness matrix (A), the coupling stiffness matrix (B), the bending stiffness matrix (D), as well as mid-plane strains, curvatures, and stresses.

It is also important to note the idealizations that CLT uses to perform its calculations. Namely, CLT assumes the lamina are perfectly bonded, the fibers are identical, linear elastic behavior is present, and there are no imperfections in the laminate. These idealizations themselves are a root cause of deviation from the MATLAB results to experimental results.

Similar to ANSYS, the inputs for CLT follow directly from the values obtained from the ROM calculations. The key outputs from the 90° and 45° laminate calculations are shown in the following figures and tables.

Reduced Stiffness Matrix Q (GPa)

$$Q = \begin{bmatrix} 17.34 & 5.31 & 0 \\ 5.31 & 17.34 & 0 \\ 0 & 0 & 1.70 \end{bmatrix}$$

Transformed Reduced Stiffness Matrix $\bar{Q}$ (GPa)

$$\bar{Q} = \begin{bmatrix} 17.34 & 5.31 & 0 \\ 5.31 & 17.34 & 0 \\ 0 & 0 & 1.70 \end{bmatrix}$$

Laminate ABD Matrix

$$ABD = \begin{bmatrix} 3.9087 \times 10^7 & 2.8868 \times 10^7 & 0 & 0 & 0 & 0 \\ 2.8868 \times 10^7 & 3.9087 \times 10^7 & 0 & 0 & 0 & 0 \\ 0 & 0 & 1.8056 \times 10^7 & 0 & 0 & 0 \\ 0 & 0 & 0 & 29.3145 & 21.6510 & 0 \\ 0 & 0 & 0 & 21.6510 & 29.3145 & 0 \\ 0 & 0 & 0 & 0 & 0 & 13.5414 \end{bmatrix}$$

$A\ [N/m], \quad B\ [N], \quad D\ [N \cdot m]$

Figure 11. CLT matrix results (90°)

Reduced Stiffness Matrix Q (GPa)

$$Q = \begin{bmatrix} 17.34 & 5.31 & 0 \\ 5.31 & 17.34 & 0 \\ 0 & 0 & 1.70 \end{bmatrix}$$

Transformed Reduced Stiffness Matrix $\bar{Q}$ (GPa)

$$\bar{Q} = \begin{bmatrix} 13.0849 & 9.6236 & 0 \\ 9.6236 & 13.0849 & 0 \\ 0 & 0 & 6.0172 \end{bmatrix}$$

$$ABD = \begin{bmatrix} 3.9087 \times 10^7 & 2.8868 \times 10^7 & 0 & 0 & 0 & 0 \\ 2.8868 \times 10^7 & 3.9087 \times 10^7 & 0 & 0 & 0 & 0 \\ 0 & 0 & 1.8056 \times 10^7 & 0 & 0 & 0 \\ 0 & 0 & 0 & 29.3145 & 21.6510 & 0 \\ 0 & 0 & 0 & 21.6510 & 29.3145 & 0 \\ 0 & 0 & 0 & 0 & 0 & 13.5414 \end{bmatrix}$$

$$A\ [N/m], \quad B\ [N], \quad D\ [N \cdot m]$$

Figure 12. CLT matrix results (45°)

	$\mathbf{E_x}$ **(GPa)**	$\mathbf{E_y}$ **(GPa)**	$\mathbf{G_{xy}}$ **(GPa)**	ν_{xy}	ν_{yx}	ε_{x0}	ε_{y0}	γ_{xy0}	$\boldsymbol{\sigma_{11}}$ **(MPa)**	$\boldsymbol{\sigma_{22}}$ **(MPa)**	$\boldsymbol{\tau_{12}}$ **(MPa)**
90°	15.73	15.73	1.7	0.306	0.306	2.504e-3	-7.663e-4	0	0	39.37	0
45°	5.92	5.92	6.02	0.7386	0.7386	6.648e-3	-4.910e-3	0	19.684	19.684	19.684

Table 3. CLT: remaining constants, stresses, strains, curvatures

Note that the Q and Qbar matrix are identical in the 90° laminate since the fiber axis (1,2) is aligned with the global axis (x,y). The B matrix being zero also confirms that the laminate is symmetrical. Similarly, the B matrix is zero in the 45° laminate, however the fibers are no longer aligned with the global axis and thus Qbar is not the same as Q. Noting a similar pattern Table x, the global property constants are the same as the fiber-direction constants for the 90° but not the 45° laminate. CLT also outputs curvatures (κ_x, κ_y, κ_{xy}), but all curvature values equal zero when performing a tensile test on symmetrical laminates since no moments are applied and there is no coupling between tension and bending.

Comparing key values between the two laminates, it follows that the longitudinal and transverse modulus are less for the 45° laminate, but the shear modulus is greater. This is directly

due to the fact that the fibers are stiff along their axis, but don't resist shear as well. In the 45° laminate, application of axial loads results in some fibers in tension and others in compression, ultimately providing great resistance to shear but less to longitudinal loads. It is also important to note the absence of shear stress in the 90° laminate but its presence in the 45° laminate, which stems from the similar idea of axial loading on 45° fibers is not fully aligned with the fiber axes.

The CLT data from MATLAB expectedly matches extremely well with the data acquired from ANSYS (see Table x (the one with ANSYS data)). Specifically, the two points of interest would be the mid-plane strain in the x-direction (ε_{x0}) as well as the stress value(s). Note that the tensile stress value obtained from ANSYS exhibits itself fully in σ_{22} for the 90° laminate, but is resolved into half its magnitude across the three stress values for the 45° laminate simply due to the angle transformation difference.

8. ROM Calculation Discrepancy

A major assumption made for the ROM calculations was that the mass of the matrix (epoxy) remained the same before and after the vacuum bagging process. In reality, this is certainly not the case since the breather fabric absorbs some of the resin during the curing process. Thus the matrix mass, and consequently the matrix volume, are less than the values used for the calculations. Specifically, for the calculations performed, Vf=0.34 and Vm=0.66. Back calculations through a tedious MATLAB series of scripts were performed to find values that should theoretically better match the true Vm (and Vf) values, and those were Vm=43.5 for the 45° laminate and Vm =0.63 for the 90° laminate. Note that there is a discrepancy between these

two values, which may stem from differences/errors in the vacuum bagging process between the two samples. In either case, the volume of the matrix is less than the value used in the ROM calculations.

9. Lab 1 Conclusions

The manufacturing and testing process yielded largely successful results, with clean demolding, no delamination or dry spots observed in either panel, and clear fracture behavior consistent with expected fiber orientation effects. However, the two panels being manufactured on separate days introduced inconsistencies in vacuum seal quality and lab temperature conditions, and the resin mass loss during vacuum bagging was not tracked, leading to an inaccurate Vf that propagated error through all theoretical predictions. The strain gauge also malfunctioned on several samples, reducing the usable dataset and limiting the statistical robustness of the experimental results. Going forward, panels should be manufactured in a single session where possible, resin mass should be measured before and after cure to capture actual Vf, and additional samples should be prepared to account for instrumentation failures during testing.

In addition to the knowledge we gained in the field of composites, this study helped us build a strong and cohesive team dynamic. All researchers took on their area of focus with pride and dedication, which was crucial for the successful culmination of our research into an in-depth report. Even on short notice, all researchers were willing and responsive to questions and discussions, which facilitated the meshing of different areas of this lab into one clear and connected summary. We hope to reinforce these strong team dynamics in project two, and will surely have strong respect for each other far beyond the end of the semester.

10. Project 2 Proposal

Our concept for project two is focused on the creation of various aerodynamic and structural components for a formula-style race car in collaboration with the Tufts Electric Racing team for the 2026 Formula Hybrid Competition. Specifically, we will design, iterate, and manufacture a nose cone and rear wing for the team's car, with the goal of minimizing part weight to create a faster car.

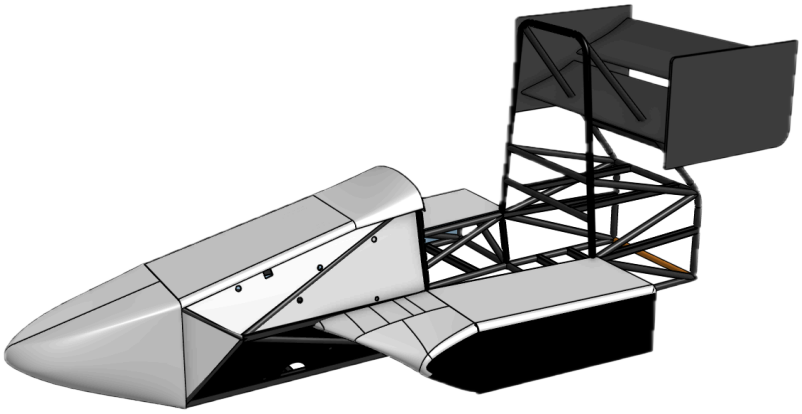

Figure 13. Assembly of Tufts Electric Racing "First Charge" FSAE Car 2026

In order to ensure these parts will withstand the forces of driving on a racetrack, ANSYS will be used to validate the structural integrity of predetermined mounting points within the composite. With this information, the design of the composite can be properly iterated to create the final parts. ANSYS will also be used to determine the appropriate thickness of the rear wing airfoils, to ensure the wing does not overdeflect or fail under high speeds due to downforce.

Some manufacturing challenges we expect to encounter will be the mold making process, as well as the size of the parts. As many of these parts have complex 3D contours, mold making likely has to be programmed on a CNC, which is costly and time consuming. This also leads to

potential faults or delays in the mold making process that must be readily planned for if something does go wrong. Due to the limited working space in the Tufts Composites Lab, some parts will be challenging to layup and seal properly, which can lead to faulty parts. This will be best remedied by proper planning and time management throughout the process of the project.

The selected materials will likely be carbon fiber or carbon kevlar fiber, both for their notable strength and stiffness to weight ratio, as well as an epoxy resin for the matrix. All parts will also be lined on the interior surface with copper foil for electrostatic grounding to comply with the rules outlined by the Formula Hybrid competition.

Our proposed timeline for the project is as follows:

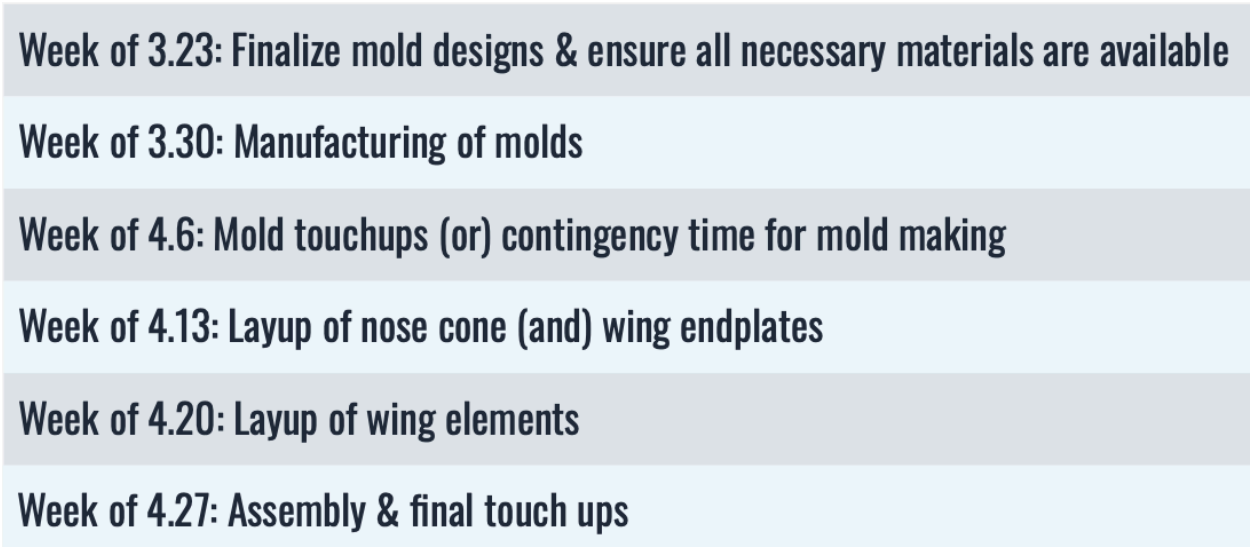

Figure 14. Proposed timeline for project two